Abdominal Radiology (2019) 44:2978–2987
https://doi.org/10.1007/s00261-019-02129-6

SPECIAL SECTION: RECTAL CANCER

Developing a prediction model based on MRI for pathological complete response after neoadjuvant chemoradiotherapy in locally advanced rectal cancer

Lijuan Wan[1] · Chongda Zhang[1] · Qing Zhao[1] · Yankai Meng[1] · Shuangmei Zou[2] · Yang Yang[1] · Yuan Liu[1] · Jun Jiang[1] · Feng Ye[1] · Han Ouyang[1] · Xinming Zhao[1] · Hongmei Zhang[1]

Published online: 20 July 2019

Abstract

Purpose The aim of this study was to build an appropriate diagnostic model for predicting pathological complete response (pCR) after neoadjuvant chemoradiotherapy (nCRT) in patients with locally advanced rectal cancer (LARC), by combining magnetic resonance imaging (MRI) parameters with clinical factors.

Methods Eighty-four patients with LARC who underwent MR examination before and after nCRT were enrolled in this study. MRI parameters including cylindrical approximated tumor volume (CATV) and relative signal intensity of tumor (rT2wSI) were measured; corresponding reduction rates (RR) were calculated; and MR tumor regression grade (mrTRG) and other conventional MRI parameters were assessed. Logistic regression with lasso regularization was performed and the appropriate prediction model for pCR was built up. An external cohort of thirty-six patients was used as the validation group for testing the model. Receiver-operating characteristic (ROC) analysis was used to assess the diagnostic performance.

Results In the development and the validation group, 17 patients (20.2%) and 11 patients (30.6%), respectively, achieved pCR. Two CATV-related parameters (CATVpost, which is the CATV measured after nCRT and CATVRR), one rT2wSI-related parameter (rT2wSIRR), and mrTRG were the most important parameters for predicting pCR and were retained in the diagnostic model. In the development group, the area under the receiver-operating characteristic curve (AUC) for predicting pCR is 0.88 [95% confidence interval (CI) 0.78–0.97, $p < 0.001$], with a sensitivity of 82.4% and a specificity of 83.6%. In the validation group, the AUC is 0.84 (95% CI 0.70–0.98, $p = 0.001$), with a sensitivity of 81.8% and a specificity of 76.0%.

Conclusion A diagnostic model including CATVpost, CATVRR, rT2wSIRR, and mrTRG was useful for predicting pCR after nCRT in patients with LARC and may be used as an effective organ-preservation strategy.

Keywords Rectal neoplasms · Magnetic resonance imaging · Magnetic resonance tumor regression grading · Neoadjuvant chemoradiotherapy · Pathological complete response

Abbreviations

ADC	Apparent diffusion coefficient
CP	Circumferential percentage
CATV	Cylindrical approximated tumor volume
CATVRR	The reduction rate of cylindrical approximated tumor volume
DTA	Distance from tumor to anal verge
EMVI	Extramural venous invasion
LARC	Locally advanced rectal cancer
MRF	Mesorectal fascia
mrTRG	Magnetic resonance tumor regression grading
nCRT	Neoadjuvant chemoradiotherapy
pCR	Pathological complete response
rT2wSI	Relative signal intensity of tumor
rT2wSIRR	The reduction rate of relative signal intensity of tumor
TME	Total mesorectal excision
TP	Tumor position

Lijuan Wan and Chongda Zhang have contributed equally to this study.

✉ Hongmei Zhang
zhanghongmei1973@163.com

Extended author information available on the last page of the article

Introduction

Neoadjuvant chemoradiotherapy (nCRT) followed by total mesorectal excision (TME) is recommended for patients with locally advanced rectal cancer (LARC) for reducing local recurrence rate [1]. Approximately, 15–27% of patients achieved pathological complete response (pCR) after nCRT [2]. These patients had excellent outcomes even though they were not treated with extensive surgery after nCRT [3, 4]. Therefore, an organ-preserving strategy such as local excision or "watch-and-wait" policy has been proposed for the patients with pCR to reduce the risk of morbidity (postoperative complications, long-term bowel, bladder and sexual dysfunction, or permanent stoma care) and mortality associated with invasive surgery [4–6].

Precise selection of patients with pCR is the key element to safely implement less invasive treatment strategies. Magnetic resonance imaging (MRI), as a noninvasive tool, is well accepted for the evaluation of rectal cancer. MR parameters, such as tumor volume, T2 signal intensity, apparent diffusion coefficient (ADC) value of tumor, and MRI-based tumor regression grading (mrTRG), were reported to be useful for the prediction of treatment response after nCRT [7–11]. However, the effect of these factors still remains controversial [12–14]. Moreover, most recent studies were merely focused on one or two MRI factors which may be insufficient for pCR prediction and for safe prescription of a patient-tailored treatment.

Therefore, the purpose of this study was to evaluate the MRI parameters along with clinical factors for the prediction of pCR. In addition, we tried to construct a diagnostic model for predicting pCR after nCRT in patients with LARC.

Materials and methods

Patients

This retrospective study was approved by our institutional ethics committee and the need for informed consent was waived. Cases with MRI-defined LARC were reviewed between October 2012 and August 2014. The following inclusion criteria were applied: (1) rectal adenocarcinoma confirmed by proctoscopic biopsy; (2) no evidence of distant metastases; (3) baseline MR examination in all patients within two weeks before nCRT; (4) surgery undergone by all patients. A total of 158 consecutive patients were enrolled. Patients were excluded if they met the following criteria: direct surgery without nCRT (n = 35), incompletion of nCRT (n = 2), no post-treatment MR examination during 4–6 weeks after nCRT (n = 14), and time interval between nCRT and surgery more than 6–8 weeks (n = 6). In addition, patients with mucinous adenocarcinoma (MAC) were also excluded (n = 17) due to distinct MR features, requiring a different assessment system for evaluating tumor treatment response to nCRT [15]. A total of 84 patients were enrolled in the study (60 males, 24 females; median age, 58 years [range, 29–82 years]) as the development group. To test the study results, the external 36 patients (21 males, 15 females; median age, 55 years [range, 30–81 years]) who met the inclusion criteria were enrolled as the validation group between January 2011 and June 2012.

Treatment and histopathological examination

All patients received nCRT at a total dose of 50 Gy, administered in fractions of 2 Gy, five times a week. Twenty-five fractions were delivered in 35 days. Capecitabine was orally administered concurrently at a dose of 1650 mg/m^2 daily for seven periods. The patients underwent surgery 6–8 weeks after nCRT

Histopathological evaluation of each specimen was performed by an experienced pathologist according to the method described by Quirke et al. [16] and TNM staging system as the gold standard. Patients with pCR were characterized by an absence of residual tumor cells in each specimen (yT0N0), and other patients were grouped to non-pCR.

MRI acquisition

MRI measurements were obtained at a 3.0T system (Signa Excite HD, GE Healthcare, USA) using an eight-element phased-array wrap-around surface coil. In our institute, all patients were routinely examined in the supine position after application of ultrasound transmission gel (60–100 ml) to highlight the tumor borders within the lumen. The imaging sequences were as follows: T2-weighted images (oblique axial, sagittal, and coronal), T1-weighted images (pelvic axial) and T2-weighted images with fat saturation (T2WI/FS). The detailed protocols are summarized in Table 1.

Imaging analysis

All MRI images were reviewed on a picture-archiving and communication system workstation (Carestream.GCRIS). Two radiologists with 17 (reader 1) and 14 (reader 2) years' experience in gastrointestinal imaging assessed the before and after nCRT MR images of the development group, blinded to the pathological and clinical details. T2-weighted images were used as the key sequence for evaluation. When the tumor could not be discerned clearly based only on T2-weighted images, other sequences were used for

Table 1 Protocols for the MR imaging sequence

Parameter	Oblique T2WI	Sagittal T2WI	Coronal T2WI	T1WI	T2WI/FS
TR	4800	4800	4800	5600	5700
TE	115	115	115	Min	85
FOV	16	24	24	34	34
Matrix	256×320	256×320	256×320	288×224	288×224
Bandwidth	41	41	41	41	31
NEX	4	4	4	2	2
Frequency direction	R/L	A/P	S/I	R/L	R/L
ETL	21	21	21	4	21
Slice thickness	3	4	4	5	5
Intersection gap	0	0.4	0.4	0.5	0.5

assistance. Tumor was defined as areas with intermediate signal intensity that is different from that of the normal rectal wall on T2-weighted images. In the development group, after all parameters were assessed independently by the two radiologists, the average of quantitative parameters was applied and the difference in qualitative parameters between reader 1 and reader 2 was unified through discussion. The third radiologist with 10 (reader 3) years' experience in gastrointestinal imaging independently assessed these parameters in the validation group. Radiologists (reader 1–3) were trained regarding the assessment criteria for all parameters before imaging evaluation. The fourth radiologist with 12 (reader 4) years' experience in gastrointestinal imaging retrospectively reviewed the before and after nCRT MR images of validation group and evaluated pCR based on his own clinical experience.

Tumor position (TP) and circumferential percentage (CP)

TP and CP were evaluated at the slice with the largest tumor dimension on oblique axial T2-weighted images before nCRT. The rectal wall was divided into four parts along two orthogonal lines that passed through the perceived center of the lumen, i.e. anterior, posterior, left lateral, and right lateral wall. Based on the location of the tumor main body revealed by TP, the specimens were divided into four groups (group 1, anterior; 2, posterior; 3, left lateral; 4, right lateral wall). According to the percentage of tumor invasion in the rectal wall revealed by CP, the specimens were divided into four groups (group 1, less than 25%; 2, 25–50%; 3, 50–75% and 4, more than 75%).

Mesorectal fascia (MRF) and extramural venous invasion (EMVI)

MRF involvement was defined as main tumor extension, tumor deposits, or suspicious lymph nodes lying within 1 mm of the mesorectal fascia and the outer border of the internal sphincter. EMVI was evaluated according to the 5-scale scoring system suggested by Smith et al. [17]. A score of 3 or 4 was considered as EMVI-positive.

Distance from tumor to anal verge (DTA)

DTA was obtained from the layer of sagittal T2-weighted images showing the maximum longitudinal length of the tumor. The distance from the inferior part of the tumor to the anal verge was defined as DTA.

Cylindrical approximated tumor volume (CATV)

The maximum tumor area (MTA) was estimated at the same slice that was used for the evaluation of TP (Fig. 1a). The region of interest (ROI) was manually drawn along the margin of the tumor, avoiding the obscure composition area, while the corresponding area was automatically calculated as MTA. The maximum tumor length (MTL) was acquired on the same section that was used for the measurement of DTA (Fig. 1b). MTA and MTL were obtained on before- and after-nCRT MR images and labeled as MTApre, MTApost, MTLpre and MTLpost, respectively.

CATV was calculated roughly as MTA×MTL, which might be more clinically practical. The CATV obtained before and after nCRT were recorded as CATVpre and CATVpost, respectively. The reduction rate of cylindrical approximated tumor volume (CATVRR) was determined correspondingly using the following equation: (CATVpre − CATVpost) × 100%/CATVpre.

Relative signal intensity of tumor (rT2wSI)

The ROI that was used for the measurement of MTA was also applied for estimating the absolute signal intensity of the tumor (Fig. 2a, b). Meanwhile, the signal intensity of the obturator internus was also obtained on the same section (Fig. 2a, b). The boundaries of tumor and obturator internus were avoided when measuring. rT2wSI was obtained using the absolute

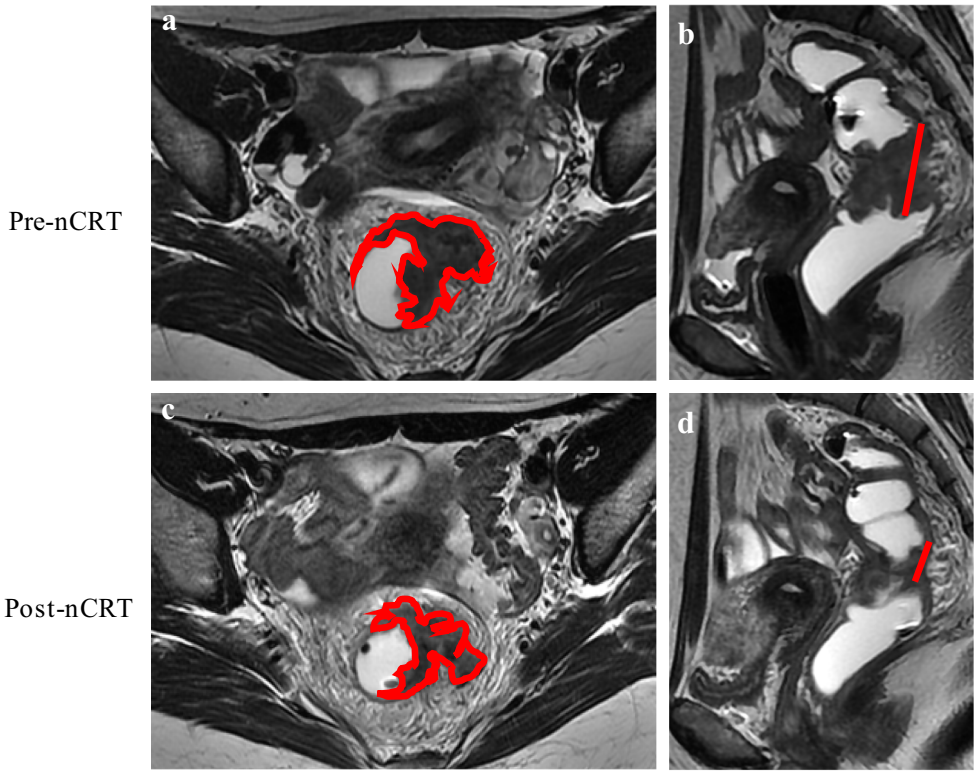

Fig. 1 **a–d**: Pre- and post-nCRT T2-weighed image sets from a 71-year-old woman with rectal cancer (yT3N2). **a** The maximum tumor area (MTA) was traced at the slice with the largest tumor dimension on the high-spatial-resolution oblique axial T2-weighted images (red curve). **b** The maximum tumor length (MTL) on the layer of sagittal T2-weighted images showing the maximum longitudinal length of the tumor (red line). **c**, **d** MTA and MTL of the same patient after nCRT

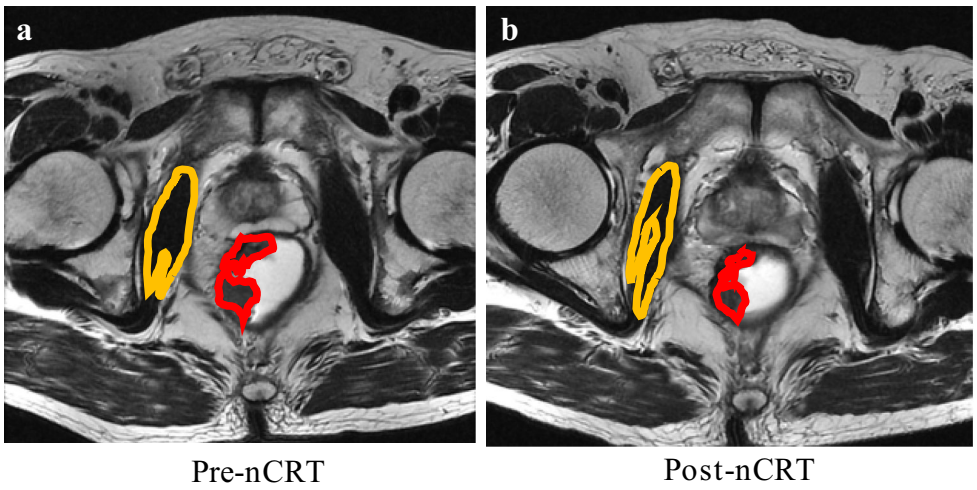

Fig. 2 **a**, **b** Pre- and post-nCRT T2-weighted image sets from a 63-year-old man with rectal cancer (yT2N0). **a** The slice with largest tumor dimension on the high-spatial-resolution oblique axial T2-weighted images was selected, the ROIs of the tumor (red curve) and the obturator muscle (yellow curve) were traced to obtain the relative signal intensity of tumor (rT2wSI). **b** rT2wSI of the same patient after nCRT

signal intensity of the tumor divided by the signal intensity of the obturator internus. Similarly, rT2wSI was measured before and after nCRT (rT2wSIpre and rT2wSIpost). The reduction rate of rT2wSI (rT2wSIRR) equals (rT2wSIpre − rT2wSIpost) × 100%/ rT2wSIpre.

Magnetic resonance tumor regression grade (mrTRG)

mrTRG was stratified into five grades as suggested by Patel et al. [18]: grade 1 = complete regression, the absence of

visible tumor signal; 2 = rare tumor signal in the context of low-signal intensity fibrosis; 3 = predominant fibrosis but obvious area of intermediate- signal-intensity tumor; 4 = residual tumor outgrowing fibrosis; 5 = no regression, absence of changes from baseline.

Statistical analysis

Univariate analysis was used to test whether a single variable has a statistically significant difference between the pCR and the non-pCR group. Q–Q plot was performed for normality test. The *t* test and the Mann–Whitney *U* test were performed for continuous variables, and the chi-square test and Fisher exact test for binary and ordinal categorical variables. Logistic regression with lasso regularization was applied for selecting the most useful parameters to build a diagnostic model from different combinations of MRI-related parameters and clinical factors using the development group data. A ten-fold cross-validation strategy was used for internal validation of the model on unseen data. The diagnostic performance of the model was expressed by the area under the ROC curve (AUC), sensitivity, and specificity. The diagnostic performance of the others' model, which was built with mrTRG, CATV-related parameters, and rT2wSI-related parameters alone, was also calculated. We tested the model on an external validation group and the AUC, sensitivity, and specificity of the validation group were calculated. The diagnostic performance of the radiologist based on experience was also calculated in the validation group. The Delong method was used to compare the AUC of the model and the others' model in the development group, and the AUC of the model and the radiologist in validation group. The intraclass correlation coefficient (ICC) was employed to estimate the interreader reproducibility of all quantitative parameters in the development group: ICC < 0.20, poor agreement; 0.21–0.40, fair; 0.41–0.60, moderate; 0.61–0.80, substantial; and > 0.80, excellent. The statistical language R version 3.5.1 (http://www.Rproject.org) was used for all statistical analyses. $P < 0.05$ was considered statistically significant.

Results

Patients

The clinical factors of the enrolled patients are presented in Table 2. Of the 84 patients in the development group, 43 patients underwent an abdominal perineal resection, 37 patients underwent a low-anterior resection, and four patients underwent a Hartman's procedure. At histopathology, 17 (20.2%) patients had a pCR (yT0N0), while 67 (79.8%) patients did not (non-pCR).

Table 2 The clinical factors of the enrolled patients in development group

	Development group		
	pCR	non-pCR	*p*
Age(years)	55±14	58±12	0.349
Gender			0.552
Male	11	49	
Female	6	18	
CEA			0.041
Normal (< 5 ng/ml)	14	37	
Abnormal (≥ 5 ng/ml)	3	30	
Type of surgery			NA
Abdominal perineal resection	10	33	
Low-anterior resection	6	31	
Hartman's procedure	1	3	

pCR Pathological complete response; *non-pCR* no pathological complete response

Univariate analysis

Regarding clinical factors, the CEA level showed a significant difference between pCR and non-pCR ($p = 0.041$) groups, while the parameters of age and gender showed no differences (Table 2).

Table 3 shows the results of univariate analysis for pCR prediction using MRI-related parameters. DTA, mrTRG, CATVpost, CATVRR, rT2wSIpost, and rT2wSIRR were proven to be statistically significant between pCR and non-pCR on univariate analysis. Other parameters (CP, TP, MRF, EMVI, CATVpre, and rT2wSIpre) showed no significant relation to pCR prediction.

The ICC values of CP, TP, MRF and all quantitative parameters were more than 0.80 and demonstrated excellent agreement between the two readers. The ICC value of EMVI and mrTRG showed a substantial or a fair agreement between the readers.

Multivariate analysis

A total of 15 variables were included in the multivariate analysis. Candidates with nonzero coefficient were screened using a lasso logistic regression model. Four parameters were retained in the diagnostic model for pCR prediction after nCRT, namely CATVpost, CATVRR, rT2wSIRR, and mrTRG. The prediction model is shown in Table 4.

Diagnostic performance

The diagnostic performance of the model for predicting pCR showed an AUC of 0.88 (95% CI 0.78–0.97, $p < 0.001$) and achieved a sensitivity of 82.4% and a

Table 3 Univariate analysis of demographics and MRI-related parameters for pCR prediction

Characteristic	pCR ($n = 17$)	non-pCR ($n = 67$)	*P* value	ICC
CP (1/2/3/4)	0/7/5/5	3/19/18/27	0.683[d]	0.917
TP (1/2/3/4)	8/1/4/4	24/9/18/16	0.860[d]	0.964
MRF (+/−)	15/2	52/15	0.503[d]	0.860
EMVI (+/−)	14/3	43/24	0.152[c]	0.669
DTA (cm)	4.77±2.47	6.44±2.58	0.019[a]	0.988
CATV				
CATVpre (cm^3)	12.82 (7.93)	14.54 (17.40)	0.258[b]	0.965
CATVpost (cm^3)	1.55 (2.20)	4.60 (5.12)	<0.001[b]	0.956
CATVRR (%)	0.88 (0.19)	0.73 (0.24)	<0.001[b]	0.915
rT2wSI				
rT2wSI pre	2.61 ± 0.46	2.45±0.43	0.178[a]	0.871
rT2wSI post	1.43 ± 0.24	1.72±0.42	0.007[a]	0.893
rT2wSIRR (%)	0.44 ±0.13	0.29±0.16	0.001[a]	0.815
mrTRG (1-2/3-5)	2/15	32/35	0.007[c]	0.330

pCR pathological complete response; *non-pCR* no pathological complete response; *CP* circumferential percentage of rectal involvement; *TP* the tumor position; *MRF* mesorectal fascia; *EMVI* extramural venous invasion; *DTA* distance to anal verge; *CATV* cylindrical approximated tumor volume; *CATVpre* cylindrical approximated tumor volume measured before nCRT; *CATVpost* cylindrical approximated tumor volume measured after nCRT; *CATVRR* cylindrical approximated tumor volume reduction rate; *rT2wSI* relative signal intensity of tumor to muscle; *rT2wSIpre* relative signal intensity of tumor to muscle measured before nCRT; *rT2wSIpost* relative signal intensity of tumor to muscle measured after nCRT; *rT2wSIRR* relative signal intensity of tumor to muscle reduction rate; *mrTRG* MR tumor regression grade

[a]The *t* test

[b]The Mann–Whitney *U* test

[c]Chi-square test

[d]The Fisher exact test

Table 4 Parameters were retained in the diagnostic model for predicting pCR

Variable	β	OR
CATVpost	− 0.051	0.950
CATVRR	1.733	5.659
rT2wSIRR	1.220	3.388
mrTRG	0.018	1.019
Intercept	− 2.875	–

CATVpost cylindrical approximated tumor volume measured after nCRT; *CATVRR* cylindrical approximated tumor volume reduction rate; *rT2wSIRR* relative signal intensity of tumor to muscle reduction rate; *mrTRG* MR tumor regression grade; *β* Regression coefficient; *OR* odds ratio

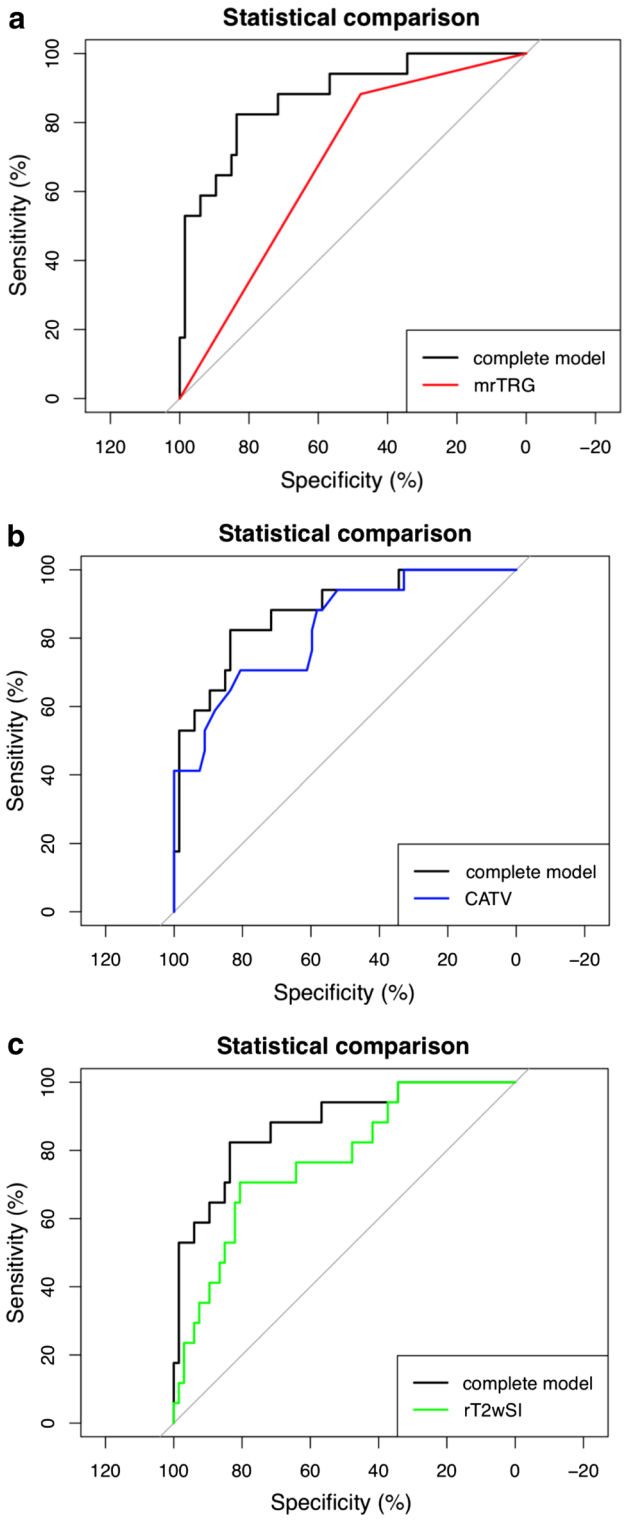

Fig. 3 **a–c** The diagnostic performance for pCR in the development group: receiver operating characteristic curve (ROC) of complete model for predicting pathological complete tumor response in locally advanced rectal cancer, AUC = 0.88 (black line); **a** ROC of mrTRG alone model, AUC = 0.68 (red line); **b** ROC of the model combining CATV-related parameters, AUC = 0.83 (blue line); **c** ROC of the model combining rT2wSI-related parameters, AUC = 0.77 (green line)

specificity of 83.6% (Fig. 3a–c). When predicting pCR using mrTRG, CATV-related parameters (CATVpre, CATVpost and CATVRR), or rT2wSI-related parameters (rT2wSIpre, rT2wSIpost and rT2wSIRR) alone, the AUC of the model including mrTRG is 0.68 (sensitivity 88.2% and specificity 47.8%) (Fig. 3a), the model combining CATV-related parameters is 0.83 (sensitivity 70.6% and specificity 80.6%) (Fig. 3b) and the model combining rT2wSI-related parameters is 0.77 (sensitivity 70.6% and specificity 80.6%) (Fig. 3c). Moreover, the AUC of the complete model was significantly greater than that using mrTRG ($p = 0.006$) and similar to the model combining CATV-related parameters ($p = 0.513$) and the model combining rT2wSI-related parameters ($p = 0.186$) (Fig. 3a–c).

Validation group

The validation group comprised 11 (30.6%) patients with pCR and 25 (69.4%) patients with non-pCR. The AUC of the validation group calculated using the model for predicting pCR is 0.84 (95% CI 0.70–0.98, $p = 0.001$), which is similar to that of the development group, with a sensitivity of 81.8% and a specificity of 76.0%, respectively. The AUC of the validation group evaluated by radiologist based on experience for predicting pCR is 0.61 (sensitivity 45.5% and specificity 76.0%). The AUC of the model was significantly greater than that of radiologist based on experience for predicting pCR ($p = 0.047$) (Fig. 4).

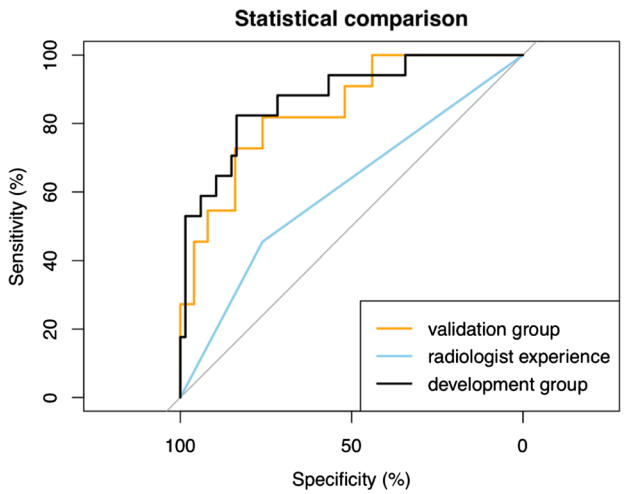

Fig. 4 The diagnostic performance for pCR in the validation group: receiver operating characteristic curve (ROC) in the validation group of a complete model for predicting pathological complete tumor response in locally advanced rectal cancer; AUC = 0.84 (orange line); ROC in validation group of radiologist experience, AUC = 0.61 (sky blue line)

Discussion

In the present study, we developed a model, which include the parameters of CATVpost, CATVRR, rT2wSIRR, and mrTRG, to predict pCR for patients with LARC. The model was validated in an external validation group yielding a good diagnostic performance for assessing pCR (AUC0.84), and showing a better diagnostic performance than radiologist based on experience as well.

For construction of a diagnostic model to predict pCR, we extracted potential parameters including MRI-related parameters and clinical factors and selected them using the lasso method to address overfitting. Our study showed that the complete model including CATVpost, CATVRR, rT2wSIRR and mrTRG, was better than assessing pCR with mrTRG alone. Moreover, although the AUCs of the model built with CATV-related parameters (CATVpre, CATVpost and CATVRR) or with rT2wSI-related parameters (rT2wSIpre, rT2wSIpost and rT2wSIRR), had no significant difference with the complete model, the complete one tended to have better sensitivity and specificity.

The estimation of tumor size before and after nCRT is an important criterion to quantify the treatment response. In contrast to one- or two-dimensional diameter measurements, tumor volume measurement easily reflects the irregular tumor shape and can identify more information of tumor size changes induced by nCRT. Many studies have reported that the post-nCRT tumor volume and tumor volumetric reduction rate, in which volume measurement was obtained by multiplying cross-sectional area by the section thickness, are valuable parameters to assess treatment response to nCRT [19–21]; however, the volume measurement method required more labor and time. In our study, we multiplied MTA by MTL to obtain a cylindrical approximated tumor volume and demonstrated that CATVpost and CATVRR also are useful in assessing pCR. Both CATVpost and CATVR were retained in the diagnostic model. Therefore, we hypothesized that CATV may be used as a surrogate for real tumor volume in busy clinical practice.

Chemoradiotherapy induces fibrosis of tumor tissue, which will lead to changes in T2-weighted signal intensity from intermediate to hypointensity. In current radiological practice, visual image evaluation of signal intensity changes is dominant, but clearly distinguishing rare residual tumor from fibrotic background is difficult. In our study, we quantified the changes in signal intensity of the lesion and used the absolute signal intensity of the tumor divided by the signal intensity of the obturator internus to remove the difference arising from MRI units. The results showed that rT2wSIRR can be used for predicting pCR and a higher rT2wSIRR meant a greater likelihood of pCR,

which was concordant with the findings of Kluza E et al [8]. In addition, rT2wSIpost showed a significant decrease in the pCR group; however, the diagnostic model failed to identify rT2wSIpost as a member for predicting pCR. This is likely because rT2wSIpost contained the partial information of rT2wSIpre while rT2wSIRR effectively excluded this information.

Assessment of mrTRG was done based on the relative proportion of residual tumor to treatment-induced fibrosis, which could be used as an imaging parameter to select patients with complete treatment response after nCRT. However, according to the aforementioned disadvantage of the visible image evaluation, one study reported the agreement between mrTRG and pathological TRG (pTRG) to be low ($k = 0.25$) [14] and another study reported that mrTRG had a wide range Kappa agreement (0.14–0.82) [22]. Siddiqui MR et al [22] suggested that enough testing and retesting were necessary before assessing mrTRG. We trained radiologists before the evaluation and divided the specimens based on mrTRG response into two groups to try to improve interreader agreement: good treatment response (mrTRG (1–2)) and poor treatment response (mrTRG (3–5)). Strong correlation was observed between mrTRG (1–2) and pCR, which was concordant with previous findings of Fayza MS et al. [23]. However, a fair agreement between the readers of mrTRG still appeared in this study. Fortunately, from the results of this study, we revealed that adding quantitative parameters, which had excellent agreement, to mrTRG can obtain a better diagnostic performance for pCR.

The parameters of CP, TP, MRF and EMVI measured before nCRT did not show enough strength for predicting pCR in our study. Interestingly, we found that DTA was significantly associated statistically with pCR and the closer distances to anal verge tend to make pCR determination easier. A hypothesis proposed that the closer the tumor was to anal verge, the less likely it was to take a geographic miss and the more likely to receive radiation therapy volumes and prescription doses [24]. Nevertheless, the explanation for DTA remains unconfirmed and other studies reported no statistical association between DTA and pCR [25, 26].

CEA is a complex glycoprotein with different glycosylations on the surface of the cell. CEA level was extracted as a laboratory test factor for the model development. This study found that lower initial CEA level showed significant statistical association with pCR on univariate analysis, which was concordant with the previous reports [26–28]. However, there were different lower initial CEA level definitions (i.e. $\leqq 3$, < 5, or < 6 ng/ml); moreover, Yang et al. [29] proposed that initial CEA level may not be used for predicting pCR. Since their diagnostic performance in predicting pCR remain controversial, both DTA and CEA level were not retained in the diagnostic model in this study.

In the study, we chose the development and validation group from two different periods of time. However, there were similar sequences and protocols for rectal MR examination between 2011 and 2014, and no major changes in the treatment regimen in patients with LARC during that period. In addition, recently, several studies have applied an external data set from different period of time for validating the model, which is more similar to the real-world clinical practice [30]. Radiomics analysis and machine learning has emerged in the field of cancer research in recent years, and radiomics analysis showed good diagnostic performance in predicting pCR after nCRT for LARC patients [31]. Nevertheless, the value of radiomics analysis and machine learning for predicting pCR needs to be further explored and verified.

This study has some certain limitations. The first limitation was the relatively small size of the development group. Therefore, we performed cross-validation for internal validation and used a new data set to evaluate the performance of the model for external validation, and a high-diagnostic performance was obtained in the validation group. However, the diagnostic value of the model should be further evaluated in a larger study. Second, diffusion-weighted imaging (DWI) and ADC values are recommended for assessing treatment response after nCRT, however, they were not included in our study because of partially limited image quality. Third, the histological differentiation was not included, due to which, about 26% of patients missed the parameters in our study. Finally, CEA level measured after nCRT (post-nCRT CEA) was not evaluated in the study because of the incomplete retrospective data. Post-CRT CEA and CEA ratio were reported to be useful for prediction of pCR in some studies [29, 32].

In conclusion, the diagnostic model including CATVpost, CATVRR, rT2wSIRR and mrTRG shows a high-predictive performance for pCR after nCRT in patients with LARC and can increase confidence in the organ-preserving strategy. Further larger studies are required to investigate the clinical applications value of the model. Moreover, future automated segmentation tools should be used for parameter assessment.

Acknowledgements The authors acknowledge Sainan Cheng and Shunan Che for their assistance with statistical analyses.

Conflict of interest All authors (Lijuan Wan, Chongda Zhang, Qing Zhao, Yankai Meng, Shuangmei Zou, Yang Yang, Yuan Liu, Jun Jiang, Feng Ye, Han Ouyang, Xinming Zhao, and Hongmei Zhang) have no conflicts of interest to be disclosed related to this article.

Author contributions Study concepts/study design, data acquisition or data analysis/interpretation, all authors; quality control of date and algorithms, Jun Jiang, Feng Ye, Han Ouyang, Hongmei Zhang; statistical analysis, Lijuan Wan, Chongda Zhang, Hongmei Zhang. drafting the article or revising it critically for important intellectual content, all author; final approval of the version to be submitted, all author.

Funding information This research is supported by the Special scientific research projects of Beijing science and technology project [Grant Number Z161100000051610]; Beijing hope marathon special fund [Grant Number LC2016A05]; Peking Union Medical College Youth Fund, the Fundamental Research Funds for the Central Universities [Grant Number 3332018078]; Beijing Hope Run Special Fund of the Cancer Foundation of China [Grant Number LC2017B18].

References

1. Sauer R, Liersch T, Merkel S, et al. (2012) Preoperative versus postoperative chemoradiotherapy for locally advanced rectal cancer: results of the German CAO/ARO/AIO-94 randomized phase III trial after a median follow-up of 11 years. Journal of clinical oncology: official journal of the American Society of Clinical Oncology 30(16):1926–1933. https://doi.org/10.1200/jco.2011.40.1836
2. Maas M, Nelemans PJ, Valentini V, et al. (2010) Long-term outcome in patients with a pathological complete response after chemoradiation for rectal cancer: a pooled analysis of individual patient data. The Lancet Oncology 11(9):835–844. https://doi.org/10.1016/s1470-2045(10)70172-8
3. Hotker AM, Tarlinton L, Mazaheri Y, et al. (2016) Multiparametric MRI in the assessment of response of rectal cancer to neoadjuvant chemoradiotherapy: A comparison of morphological, volumetric and functional MRI parameters. European Radiology 26(12):4303–4312. https://doi.org/10.1007/s00330-016-4283-9
4. Renehan AG, Malcomson L, Emsley R, et al. (2016) Watch-and-wait approach versus surgical resection after chemoradiotherapy for patients with rectal cancer (the OnCoRe project): a propensity-score matched cohort analysis. The Lancet Oncology 17(2):174–183. https://doi.org/10.1016/s1470-2045(15)00467-2
5. Sartori CA, Sartori A, Vigna S, Occhipinti R, Baiocchi GL (2011) Urinary and sexual disorders after laparoscopic TME for rectal cancer in males. Journal of gastrointestinal surgery: official journal of the Society for Surgery of the Alimentary Tract 15(4):637–643. https://doi.org/10.1007/s11605-011-1459-0
6. Braendengen M, Tveit KM, Bruheim K, et al. (2011) Late patient-reported toxicity after preoperative radiotherapy or chemoradiotherapy in nonresectable rectal cancer: results from a randomized Phase III study. International journal of radiation oncology, biology, physics 81(4):1017–1024. https://doi.org/10.1016/j.ijrobp.2010.07.007
7. Tarallo N, Angeretti MG, Bracchi E, et al. (2018) Magnetic resonance imaging in locally advanced rectal cancer: quantitative evaluation of the complete response to neoadjuvant therapy. Polish journal of radiology 83:e600–e609. https://doi.org/10.5114/pjr.2018.81156
8. Kluza E, Rozeboom ED, Maas M, et al. (2013) T2 weighted signal intensity evolution may predict pathological complete response after treatment for rectal cancer. European radiology 23(1):253–261. https://doi.org/10.1007/s00330-012-2578-z
9. Enkhbaatar NE, Inoue S, Yamamuro H, et al. (2018) MR Imaging with Apparent Diffusion Coefficient Histogram Analysis: Evaluation of Locally Advanced Rectal Cancer after Chemotherapy and Radiation Therapy. Radiology 288(1):129–137. https://doi.org/10.1148/radiol.2018171804
10. Battersby NJ, Dattani M, Rao S, et al. (2017) A rectal cancer feasibility study with an embedded phase III trial design assessing magnetic resonance tumour regression grade (mrTRG) as a novel biomarker to stratify management by good and poor response to chemoradiotherapy (TRIGGER): study protocol for a randomised controlled trial. Trials 18(1):394. https://doi.org/10.1186/s13063-017-2085-2
11. Lambregts DMJ, Boellaard TN, Beets-Tan RGH (2019) Response evaluation after neoadjuvant treatment for rectal cancer using modern MR imaging: a pictorial review. Insights into imaging 10(1):15. https://doi.org/10.1186/s13244-019-0706-x
12. Kim YH, Kim DY, Kim TH, et al. (2005) Usefulness of magnetic resonance volumetric evaluation in predicting response to preoperative concurrent chemoradiotherapy in patients with resectable rectal cancer. International journal of radiation oncology, biology, physics 62(3):761–768. https://doi.org/10.1016/j.ijrobp.2004.11.005
13. Bernier L, Balyasnikova S, Tait D, Brown G (2018) Watch-and-Wait as a Therapeutic Strategy in Rectal Cancer. Current colorectal cancer reports 14(2):37–55. https://doi.org/10.1007/s11888-018-0398-5
14. Sclafani F, Brown G, Cunningham D, et al. (2017) Comparison between MRI and pathology in the assessment of tumour regression grade in rectal cancer. Br J Cancer 117(10):1478–1485. https://doi.org/10.1038/bjc.2017.320
15. Park SH, Lim JS, Lee J, et al. (2017) Rectal Mucinous Adenocarcinoma: MR Imaging Assessment of Response to Concurrent Chemotherapy and Radiation Therapy-A Hypothesis-generating Study. Radiology 285(1):124–133. https://doi.org/10.1148/radiol.2017162657
16. Quirke P, Durdey P, Dixon MF, Williams NS (1986) Local recurrence of rectal adenocarcinoma due to inadequate surgical resection. Histopathological study of lateral tumour spread and surgical excision. Lancet (London, England) 2 (8514):996-999
17. Smith NJ, Barbachano Y, Norman AR, et al. (2008) Prognostic significance of magnetic resonance imaging-detected extramural vascular invasion in rectal cancer. The British journal of surgery 95(2):229–236. https://doi.org/10.1002/bjs.5917
18. Patel UB, Taylor F, Blomqvist L, et al. (2011) Magnetic resonance imaging-detected tumor response for locally advanced rectal cancer predicts survival outcomes: MERCURY experience. Journal of clinical oncology: official journal of the American Society of Clinical Oncology 29(28):3753–3760. https://doi.org/10.1200/jco.2011.34.9068
19. Neri E, Guidi E, Pancrazi F, et al. (2015) MRI tumor volume reduction rate vs tumor regression grade in the pre-operative re-staging of locally advanced rectal cancer after chemo-radiotherapy. European journal of radiology 84(12):2438–2443. https://doi.org/10.1016/j.ejrad.2015.08.008
20. Yeo SG, Kim DY, Park JW, et al. (2012) Tumor volume reduction rate after preoperative chemoradiotherapy as a prognostic factor in locally advanced rectal cancer. International journal of radiation oncology, biology, physics 82(2):e193–199. https://doi.org/10.1016/j.ijrobp.2011.03.022
21. Seierstad T, Hole KH, Groholt KK, et al. (2015) MRI volumetry for prediction of tumour response to neoadjuvant chemotherapy followed by chemoradiotherapy in locally advanced rectal cancer. The British journal of radiology 88(1051):20150097. https://doi.org/10.1259/bjr.20150097
22. Siddiqui MR, Gormly KL, Bhoday J, et al. (2016) Interobserver agreement of radiologists assessing the response of rectal cancers to preoperative chemoradiation using the MRI tumour regression grading (mrTRG). Clinical radiology 71(9):854–862. https://doi.org/10.1016/j.crad.2016.05.005
23. Fayaz MS, Demian GA, Fathallah WM, et al. (2016) Significance of Magnetic Resonance Imaging-Assessed Tumor Response for Locally Advanced Rectal Cancer Treated With Preoperative Long-Course Chemoradiation. Journal of global oncology 2(4):216–221. https://doi.org/10.1200/jgo.2015.001479
24. Yu SK, Tait D, Chau I, Brown G (2013) MRI predictive factors for tumor response in rectal cancer following neoadjuvant chemoradiation therapy–implications for induction chemotherapy?

International journal of radiation oncology, biology, physics 87(3):505–511. https://doi.org/10.1016/j.ijrobp.2013.06.2052
25. Garland ML, Vather R, Bunkley N, Pearse M, Bissett IP (2014) Clinical tumour size and nodal status predict pathologic complete response following neoadjuvant chemoradiotherapy for rectal cancer. International journal of colorectal disease 29(3):301–307. https://doi.org/10.1007/s00384-013-1821-7
26. Wallin U, Rothenberger D, Lowry A, Luepker R, Mellgren A (2013) CEA - a predictor for pathologic complete response after neoadjuvant therapy for rectal cancer. Diseases of the colon and rectum 56(7):859–868. https://doi.org/10.1097/DCR.0b013e31828e5a72
27. Huh JW, Kim HR, Kim YJ (2013) Clinical prediction of pathological complete response after preoperative chemoradiotherapy for rectal cancer. Diseases of the colon and rectum 56(6):698–703. https://doi.org/10.1097/DCR.0b013e3182837e5b
28. Armstrong D, Raissouni S, Price Hiller J, et al. (2015) Predictors of Pathologic Complete Response After Neoadjuvant Treatment for Rectal Cancer: A Multicenter Study. Clinical colorectal cancer 14(4):291–295. https://doi.org/10.1016/j.clcc.2015.06.001
29. Yang KL, Yang SH, Liang WY, et al. (2013) Carcinoembryonic antigen (CEA) level, CEA ratio, and treatment outcome of rectal cancer patients receiving pre-operative chemoradiation and surgery. Radiation oncology (London, England) 8:43. https://doi.org/10.1186/1748-717x-8-43
30. Kim S, Han K, Seo N, et al. (2018) T2-weighted signal intensity-selected volumetry for prediction of pathological complete response after preoperative chemoradiotherapy in locally advanced rectal cancer. European radiology 28(12):5231–5240. https://doi.org/10.1007/s00330-018-5520-1
31. Liu Z, Zhang XY, Shi YJ, et al. (2017) Radiomics Analysis for Evaluation of Pathological Complete Response to Neoadjuvant Chemoradiotherapy in Locally Advanced Rectal Cancer. Clinical cancer research: an official journal of the American Association for Cancer Research 23(23):7253–7262. https://doi.org/10.1158/1078-0432.ccr-17-1038
32. Saito G, Sadahiro S, Ogimi T, et al. (2018) Relations of Changes in Serum Carcinoembryonic Antigen Levels before and after Neoadjuvant Chemoradiotherapy and after Surgery to Histologic Response and Outcomes in Patients with Locally Advanced Rectal Cancer. Oncology 94(3):167–175. https://doi.org/10.1159/000485511

Affiliations

Lijuan Wan[1] · Chongda Zhang[1] · Qing Zhao[1] · Yankai Meng[1] · Shuangmei Zou[2] · Yang Yang[1] · Yuan Liu[1] · Jun Jiang[1] · Feng Ye[1] · Han Ouyang[1] · Xinming Zhao[1] · Hongmei Zhang[1]

Lijuan Wan
lijuanwan1993@163.com

Chongda Zhang
charlotte.zcd0102@gmail.com

Qing Zhao
zq_pumc@163.com

Yankai Meng
mengyankai@126.com

Shuangmei Zou
smzou@hotmail.com

Yang Yang
yangyangpumc@126.com

Yuan Liu
Liuyuan9348@sina.com

Jun Jiang
jiangjuncams@163.com

Feng Ye
13810786957@163.com

Han Ouyang
houybj@126.com

Xinming Zhao
xinmingzh@sina.com

[1] Department of Radiology, National Cancer Center/National Clinical Research Center for Cancer/Cancer Hospital, Chinese Academy of Medical Sciences and Peking Union Medical College, #17 Panjiayuan Nanli, Chaoyang District, Beijing 100021, China

[2] Department of Pathology, National Cancer Center/National Clinical Research Center for Cancer/Cancer Hospital, Chinese Academy of Medical Sciences and Peking Union Medical College, #17 Panjiayuan Nanli, Chaoyang District, Beijing 100021, China